JHEP

Published for SISSA by Springer

Received: January 25, 2019
Revised: June 13, 2019
Accepted: August 20, 2019
Published: September 6, 2019

Almost inert Higgs bosons at the LHC

Christina Gao,[a] **Markus A. Luty**[b] **and Nicolás A. Neill**[c]

[a] *Theoretical Physics Department, Fermilab, Kirk Road and Pine Street, Batavia, IL, U.S.A.*
[b] *Center for Quantum Mathematics and Physics(QMAP), University of California Davis, One Shields Avenue, Davis, CA, U.S.A.*
[c] *Department of Physics and CCTVal, Universidad T écnica Federico Santa María, Av. España 1680, Casilla 110-V, Valparaíso, Chile*

E-mail: cgaophysics@gmail.com, markusluty@gmail.com, nicolas.neill@gmail.com

Abstract: Non-minimal Higgs sectors are strongly constrained by the agreement of the measured couplings of the 125 GeV Higgs with Standard Model predictions. This agreement can be explained by an approximate $\mathbb{Z}_2$ symmetry under which the additional Higgs bosons are odd. This allows the additional Higgs bosons to be approximately inert, meaning that they have suppressed VEVs and suppressed mixing with the Standard Model Higgs. In this case, single production of the new Higgs bosons is suppressed, but electroweak pair production is unsuppressed. We study the phenomenology of a minimal 2 Higgs doublet model that realizes this scenario. In a wide range of parameters, the phenomenology of the model is essentially fixed by the masses of the exotic Higgs bosons, and can therefore be explored systematically. We study a number of different plausible signals in this model, and show that several LHC searches can constrain or discover additional Higgs bosons in this parameter space. We find that the reach is significantly extended at the high luminosity LHC.

Keywords: Beyond Standard Model, Higgs Physics

ArXiv ePrint: 1812.08179

https://doi.org/10.1007/JHEP09(2019)043

JHEP09(2019)043

Contents

JHEP09(2019)043

1 Introduction

The discovery of the 125 GeV Higgs boson at the LHC [1, 2] has been rapidly followed by an impressive program of measurement of Higgs couplings that tells us that the Higgs couplings are consistent with Standard Model predictions at the 10% level [3–5]. Further improving the Higgs coupling measurements is an important part of the ongoing physics program at the LHC and future colliders. An important complementary probe of the Higgs sector are direct searches for additional Higgs bosons. Additional Higgs multiplets are intrinsic to many extensions of the Standard Model that address the problem of naturalness, such as supersymmetry or composite Higgs models. In addition, from a purely phenomenological point of view, it is important to experimentally constrain non-minimal Higgs sectors that could play a role in electroweak symmetry breaking and the generation of elementary particle masses without reference to specific models of naturalness.

The consistency of the observed Higgs couplings with the Standard Model strongly constrain the possibilities for discovery of additional Higgs bosons. The simplest explanation for this consistency is that any additional Higgs multiplets have large positive electroweak-preserving mass terms. These models have a "decoupling limit" where the quadratic terms of the new Higgs fields get large, with other couplings held fixed [6, 7]. In this limit, the physical masses of the new Higgs bosons becomes large, and their effects decouple at low energies. Probing additional Higgs bosons near the decoupling limit is therefore very difficult.

Another limit of multi-Higgs models that is often studied in the literature is the "alignment limit" where the lightest CP even physical Higgs boson h is closely aligned with the VEV in the multi-Higgs field space [7, 12]. The decoupling limit implies the alignment limit,

but alignment does not require the new Higgs bosons to be heavy. Alignment without decoupling is not guaranteed by any symmetry, and is therefore an accidental (or fine-tuned) property of the Higgs potential. The alignment limit has a distinctive phenomenology. The approximate alignment of the 125 GeV mass eigenstate h with the Higgs VEV guarantees that the couplings hVV ($V = W, Z$) are close to the Standard Model values. Since these are among the most precisely measured Higgs couplings, this partially explains the Standard-Model-like nature of the observed Higgs bosons. The alignment limit implies that couplings of the form HVV are suppressed, where H denotes a new Higgs boson. However, the couplings Hff (f = fermion) are allowed to be unsuppressed, so one searches for signals involving the heavies fermions t, b, and τ [12–14].

In this paper we consider a simple symmetry explanation for the Standard-Model like couplings of the 125 GeV Higgs that allows additional Higgs bosons to be light. We assume that there are additional Higgs doublets that are odd under an approximate $\mathbb{Z}_2$ symmetry, while all Standard Model fields (including the Standard Model Higgs doublet) are even under $\mathbb{Z}_2$. We first consider the limit where the $\mathbb{Z}_2$ symmetry is exact, and then include small explicit breaking. First, note that the Yukawa couplings of the additional Higgs doublets to Standard Model fermions are forbidden by $\mathbb{Z}_2$ symmetry. Next we consider the couplings of the Higgs bosons to vector bosons. We assume that the $\mathbb{Z}_2$ odd Higgs fields have positive quadratic terms, so that they have vanishing VEV, and the $\mathbb{Z}_2$ symmetry is not spontaneously broken. In this case the $\mathbb{Z}_2$-even and $\mathbb{Z}_2$-odd Higgs bosons do not mix, and the Standard Model Higgs doublet is entirely responsible for electroweak symmetry breaking. In this case, the vector couplings of the $\mathbb{Z}_2$ even Higgs boson are the same as in the Standard Model, so the $\mathbb{Z}_2$ symmetry gives a limit where the Higgs is naturally Standard Model-like. In this scenario, the additional Higgs bosons are called "inert" because they do not contribute to electroweak symmetry breaking [15, 16]. In the inert limit, the lightest $\mathbb{Z}_2$ odd particle is stable, and may be dark matter [17–25].

We consider the case where the $\mathbb{Z}_2$ symmetry is approximate, so the new Higgs bosons are only approximately inert. We will assume that all $\mathbb{Z}_2$ breaking terms are suppressed by a small dimensionless parameter ϵ. The parameter ϵ then suppresses single production of the new Higgs bosons, as well as their decays. Therefore, any deviation of the 125 GeV couplings to vectors or fermions from the Standard Model prediction is suppressed by ϵ, and the observed Higgs is naturally Standard Model-like.

The focus of this paper is on the collider signatures of these "almost inert" Higgs bosons. Standard searches for exotic Higgs particles at the LHC rely on single production of the Higgs particles, which is suppressed by ϵ in this scenario. For moderate values of ϵ (roughly $\epsilon \lesssim 0.1$) these searches are completely ineffective due to low production cross-sections. However, couplings of the form VHH ($V = W, Z, \gamma$, H = exotic Higgs) are fixed by gauge invariance, and are unsuppressed in the inert limit. These are therefore the main production mode for the new Higgs particles. The decay of the new Higgs bosons to Standard Model particles is also suppressed by ϵ. This means that heavier $\mathbb{Z}_2$ odd Higgs bosons will preferentially decay weakly to lighter $\mathbb{Z}_2$ odd Higgs bosons, followed by a slower decay of the lightest $\mathbb{Z}_2$ odd particle to Standard Model particles. This leads to cascade decays with multiple Standard Model particles in the final states. Although the last stage

JHEP09(2019)043

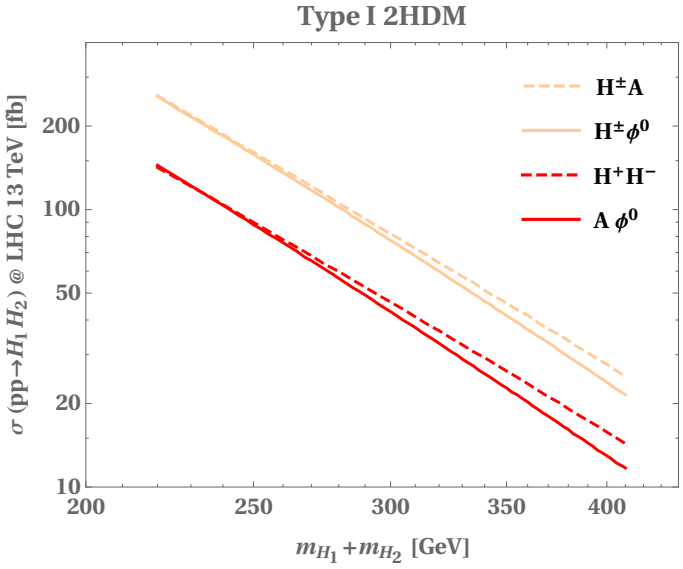

Figure 1. Production cross section for pairs of exotic Higgs bosons as a function of the total mass of the final state at LHC 13 TeV. Each curve corresponds to $\sigma^{\rm LO}_{pp\to V\to H_1H_2}$, where $V = W^\pm, Z$ as appropriate. For $H^\pm A$ we consider $m_{H^\pm} = m_A$. For $H^\pm\phi^0$ and $A\phi^0$ the cross section depends on two independent masses; we choose $m_{H^\pm} = m_A = 110$ GeV and vary m_{ϕ^0}. The cross sections were obtained with MadGraph [32].

of the decays is suppressed by ϵ, it will still be prompt as long as $\epsilon \gtrsim 10^{-4}$ (for masses of the additional scalars $\gtrsim 200\,\text{GeV}$).[1] Thus, for many orders of magnitude in the $\mathbb{Z}_2$ breaking parameter ($10^{-4} \lesssim \epsilon \lesssim 10^{-1}$) the phenomenology is dominated by prompt cascade decays. For ϵ's less than $\mathcal{O}(10^{-4})$, the approximately $\mathbb{Z}_2$-odd scalars become long-lived, so displaced vertices searches can be relevant in this regime (e.g. [26–28]). Here we limit ourselves to the prompt case, leaving the potential of displaced vertices searches for future work.

In fact, the phenomenology of this model is almost completely determined by the masses of the $\mathbb{Z}_2$-odd Higgs particles, i.e., the charged Higgs $H^\pm$, the neutral CP-even Higgs ϕ^0 and the neutral CP-odd Higgs A. The $\mathbb{Z}_2$ symmetry allows electroweak symmetry violating mass splittings within the additional Higgs multiplets. (These arise from $\mathbb{Z}_2$ invariant terms in the Higgs potential such as $|H_1^\dagger H_2|^2$, where $H_{1,2}$ are the $\mathbb{Z}_2$ even and odd Higgs doublets, respectively.) The leading production process for the new Higgs bosons is pair production from a virtual W, Z, or γ, namely[2]

$$W^* \to H^\pm\phi^0, \quad W^* \to H^\pm A, \quad Z^*/\gamma^* \to H^+H^-, \quad Z^* \to A\phi^0. \tag{1.1}$$

The production rate for these processes is fixed by gauge invariance, and the rates at the LHC are shown in figure 1. The heavier new Higgs particles will generically have cascade decays to lighter members of the new Higgs multiplet by emitting a (possibly virtual) W or Z. These decays are not suppressed by ϵ, and therefore generically dominate over decays

[1] See table 8 for a numerical example of the values of ϵ required to have prompt decays for different masses of the additional scalars.

[2] We denote the Standard Model Higgs doublet by h^0 and the CP-even $\mathbb{Z}_2$ odd Higgs boson by ϕ^0.

JHEP09(2019)043

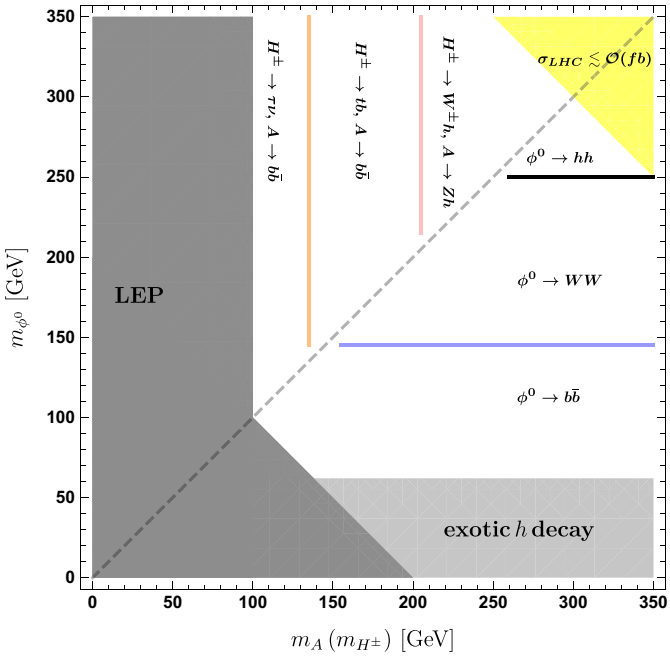

Figure 2. Dominant decay modes for $H^\pm(A)$ and ϕ^0, assuming in each case it is the lightest $\mathbb{Z}_2$ odd Higgs boson. A rough estimate of LEP bounds and LHC reach are shown in dark grey and yellow, respectively. See text for additional details.

to Standard Model states. The lightest additional Higgs then has a "slow" decay only through $\mathbb{Z}_2$ violating couplings. These can be thought of as arising from mixing with the Standard Model Higgs, and therefore go to the heaviest kinematically accessible Standard Model state. This gives rise to a rich set of many-particle final states featuring the heaviest Standard Model particles: t, h, Z, W, b, and τ.

The decay cascades are generally dominated by a single decay mode at each stage of the decay, so the signal is determined completely by the masses of the new Higgs bosons. The lightest $\mathbb{Z}_2$ odd Higgs boson decays to the heaviest kinematically available Standard Model particles. Weak production of $\mathbb{Z}_2$ odd Higgs bosons can give $H^\pm A^0$, H^+H^-, $\phi^0 H^\pm$, or $\phi^0 A^0$. These then cascade decay down to the lightest $\mathbb{Z}_2$ odd Higgs boson, generating a state with one or more vector bosons (W and/or Z) plus $\phi^0\phi^0$, H^+H^- or A^0A^0. The lightest $\mathbb{Z}_2$-odd Higgs boson then decays to Standard Model particles. Because these decays occur *via* mixing with the Standard Model Higgs, these decays are to the heaviest kinematically accessible Standard Model final state. These decays are summarized in figure 2, which also shows an estimate of the region where LEP is sensitive to the $\mathbb{Z}_2$-odd Higgs bosons. LEP can directly produce $\phi^0 A$ and H^+H^- *via* Z^*/γ^*, so it can probe the region where these states are kinematically available. The actual limits (see refs. [29, 30]) are slightly weaker than the estimate in the figure. Other constraints might come from $h \to \gamma\gamma$. Charged Higgs loop can potentially give a large contribution to this decay. As explained in the appendix, the almost inert Higgs corresponds to a large $\tan\beta$ limit of the type-I 2HDM. As shown in ref. [31], in this limit there are no any other constraints excepting the ones

JHEP09(2019)043

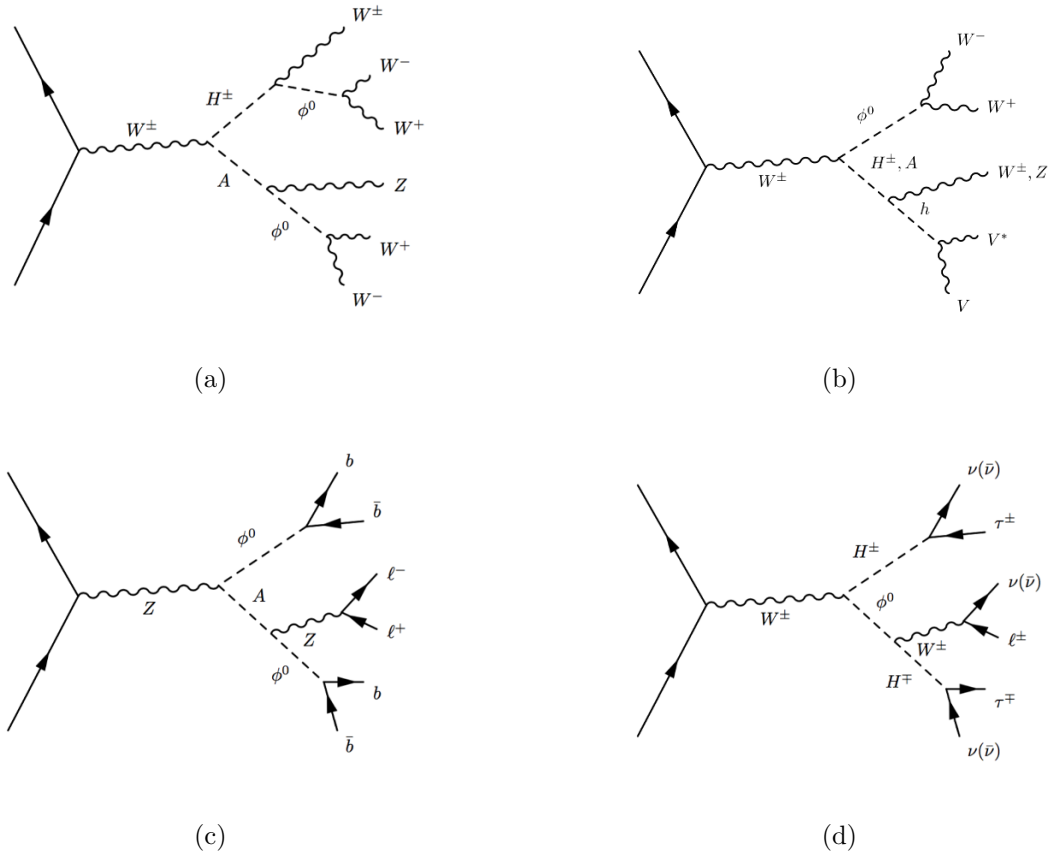

Figure 3. Examples of signal topologies that give rise to multi-lepton final states.

from LEP. In addition, figure 2 gives a rough indication of the LHC reach for this model by showing the parameter space where the LHC production rate for a pair of $\mathbb{Z}_2$-odd Higgs bosons becomes smaller than ~ 1 fb. We also restrict ourselves to masses of ϕ^0 in the range

$$62.5 \text{ GeV} < m_{\phi^0} < 250 \text{ GeV} \tag{1.2}$$

to avoid the processes $\phi^0 \to hh$ and $h \to \phi^0\phi^0$. Processes involving $\phi^0 \to hh$ will be very challenging due to the low rate. The process $h \to \phi^0\phi^0$ can become important when it is kinematically accessible, therefore it is constrained by exotic h_{SM} decays [8–11]. Moreover, the $h \to \phi^0\phi^0$ decay width depends on the parameters of the full Higgs potential. Given that in this work we wish to investigate the phenomenology dictated by introducing a small $\mathbb{Z}_2$-breaking effect, we leave this model-dependent channel for future work.

We focus on the white region in figure 2, which illustrates the parameter space we are probing. The fact that this parameter space can be represented on a 2-dimensional plot means that the phenomenology of this scenario can be explored systematically.

We have investigated a large number of processes in this model that may be possible to probe at the LHC. The results of the investigation are summarized in section 4 (tables 5, 6, and 7). For optimistic benchmark models, there are many decay modes where a 5σ discov-

JHEP09(2019)043

ery is possible with $300\,\text{fb}^{-1}$. We will show below that there is significant additional parameter space that can be probed by the high luminosity LHC ($3000\,\text{fb}^{-1}$). The most effective searches are multi-lepton channels, due to relatively low Standard Model backgrounds. Illustrative event topologies leading to multi-lepton final states are shown in figure 3. Multilepton searches are standard parts of the LHC search program, so this establishes that this model will be probed by new LHC data. In addition, we identify one case where a novel search is sensitive, involving a lepton pair (opposite sign, same flavor) plus 3 b jets.

This paper is organized as follows. In section 2 we give additional details of our benchmark model and its parameter space. In section 3 we give details of several benchmark studies. Section 4 contains our conclusions, where we give projections of the search reach for both $300\,\text{fb}^{-1}$ and $3000\,\text{fb}^{-1}$ at the LHC.

2 The model

We consider a model with 2 Higgs doublets H_1, H_2 with an approximate $\mathbb{Z}_2$ symmetry

$$H_1 \mapsto H_1, \qquad H_2 \mapsto -H_2. \tag{2.1}$$

In the $\mathbb{Z}_2$ symmetry limit, the Higgs potential is given by

$$\begin{aligned} V_0 = {} & m_1^2|H_1|^2 + m_2^2|H_2|^2 + \frac{1}{2}\lambda_1|H_1|^4 + \frac{1}{2}\lambda_2|H_2|^4 \\ & + \lambda_3|H_1|^2|H_2|^2 + \lambda_4|H_1^\dagger H_2|^2 + \frac{1}{2}\lambda_5\left[(H_1^\dagger H_2)^2 + \text{h.c.}\right] \end{aligned} \tag{2.2}$$

All couplings can be chosen real by rephasing $H_{1,2}$, so the potential of model naturally conserves CP [7]. Note that the $\lambda_{3,4,5}$ terms can give unsuppressed mass splittings in the H_2 multiplet even in the $\mathbb{Z}_2$ symmetry limit. We could even take the limit $m_2^2 \to 0$, in which case all of the mass of the exotic Higgs bosons comes from electroweak symmetry breaking. In particular, the term $|H_1|^2|H_2|^2$ contributes an electroweak-preserving mass for H_2, which does not give rise to precision electroweak observables such as S and T. The fact that this mass comes from electroweak breaking is instead reflected in the fact that H_2 has large couplings to H_1. Such large Higgs couplings are therefore the smoking gun signal of this kind of non-decoupling electroweak symmetry breaking. This particularly motivates the study of triple Higgs couplings in this class of models. We leave this study for future work.

We assume that $m_2^2 > 0$, so that in the $\mathbb{Z}_2$ symmetry limit only H_1 gets a VEV. We then have

$$\begin{aligned} v^2 &= -\frac{2m_1^2}{\lambda_1}, \\ m_h^2 &= \lambda_1 v^2, \\ m_{\phi^0}^2 &= m_2^2 + \frac{1}{2}(\lambda_3 + \lambda_4 + \lambda_5)v^2, \\ m_A^2 &= m_2^2 + \frac{1}{2}(\lambda_3 + \lambda_4 - \lambda_5)v^2, \\ m_{H^\pm}^2 &= m_2^2 + \frac{1}{2}\lambda_3 v^2, \end{aligned} \tag{2.3}$$

JHEP09(2019)043

where $\phi^0, A, H^\pm$ are the physical fields that reside in H_2. A big mass splitting in m_A and $m_{H^\pm}$ violates custodial symmetry, which is severely constrained by electroweak precision tests. Therefore, from now on, we work in the custodial symmetry limit $m_A = m_{H^\pm}$, which implies that $\lambda_4 = \lambda_5$.

We also include $\mathcal{O}(\epsilon)$ terms that break $\mathbb{Z}_2$:

$$\begin{aligned}\Delta V = {} & \Delta m^2 (H_1^\dagger H_2 + \text{h.c.}) \\ & + \Delta\lambda |H_1|^2 (H_1^\dagger H_2 + \text{h.c.}) + \Delta\lambda' |H_2|^2 (H_1^\dagger H_2 + \text{h.c.})\end{aligned} \tag{2.4}$$

Not all of the couplings in eqs. (2.2) and (2.4) are important for phenomenology. This is because $\langle H_2 \rangle = \mathcal{O}(\epsilon)$, and we are not interested in terms with more than 2 Higgs fields. The effects of λ_2 and $\Delta\lambda'$ are therefore suppressed by ϵ, and we can neglect them to get an overview of the phenomenology. (We can think of H_2 as "small.") Since we also set $\lambda_4 = \lambda_5$, we effectively have 7 parameters instead of 10:

$$v,\ m_h^2,\ m_{\phi^0}^2,\ m_A^2,\ \lambda_3,\ \Delta m^2,\ \Delta\lambda. \tag{2.5}$$

The first two parameters are of course fixed by experiment to be $m_h = 125\,\text{GeV}$ and $v = 246\,\text{GeV}$, leaving 5 free parameters. However, we will show that for small ϵ the phenomenology is essentially determined by the mass spectrum of the new Higgs bosons.

Production of $\mathbb{Z}_2$ odd Higgs bosons comes from the couplings such as $g_{ZA\phi^0}$, $g_{ZH^+H^-}$, and $g_{W^+H^-\phi^0}$, which are fixed by gauge invariance. Decays of heavier $\mathbb{Z}_2$ odd Higgs bosons to lighter $\mathbb{Z}_2$ odd Higgs bosons are controlled by the same couplings. The only additional couplings that we need are the ones that determine the decay of the $\mathbb{Z}_2$ odd Higgs bosons to the $\mathbb{Z}_2$ even Higgs bosons and Standard Model vector bosons. For these we must consider the minimization of the Higgs potential.

We define the physical fields $h, \phi^0, A, H^\pm$ in terms of the fields with the approximate the $\mathbb{Z}_2$ symmetry:

$$H_i = \begin{pmatrix} H_i^+ \\ \frac{1}{\sqrt{2}}(\tilde{v}_i + h_i + iA_i) \end{pmatrix}, \qquad i = 1, 2, \tag{2.6}$$

where $\tilde{v}_i, h_i, A_i, H_i^+$ are the VEV, CP-even neutral, CP-odd neutral and charged components in each doublet. The physical pseudoscalar field is then given by

$$A = A_2 + \epsilon_A A_1 + \mathcal{O}(\epsilon^2), \tag{2.7}$$

with

$$\epsilon_A = -\frac{\tilde{v}_2}{v} = O(\epsilon), \tag{2.8}$$

where $\tilde{v}_2 \equiv \langle H_2 \rangle$. The physical scalars are

$$\begin{pmatrix} h \\ \phi^0 \end{pmatrix} = \begin{pmatrix} 1 & \epsilon_h \\ -\epsilon_h & 1 \end{pmatrix} \begin{pmatrix} h_1 \\ h_2 \end{pmatrix} + \mathcal{O}(\epsilon^2), \tag{2.9}$$

JHEP09(2019)043

with

$$\epsilon_h = \frac{1}{m_h^2 - m_{\phi^0}^2}\left[\frac{\tilde{v}_2}{v}(m_{\phi^0}^2 - 2m_{H^\pm}^2 + \lambda_3 v^2) + \Delta\lambda v^2\right] = O(\epsilon). \tag{2.10}$$

Using standard results from 2 Higgs doublet models, together with $g_{h_1VV} \propto v_1$ and (2.8), we then obtain the interaction vertices that control the decays of the lightest $\mathbb{Z}_2$ odd Higgs:

$$\epsilon_V \frac{m_Z}{v}(p_A + p_h)^\mu Z_\mu A h \tag{2.11a}$$

$$i\epsilon_V \frac{m_W}{v}(p_{H^\pm} + p_h)^\mu W_\mu^\mp H^\pm h, \tag{2.11b}$$

$$\epsilon_V \frac{m_V^2}{v}\phi(Z^\mu Z_\mu + 2W^{+\mu}W_\mu^-) \tag{2.11c}$$

where

$$\epsilon_V = \epsilon_A + \epsilon_h = O(\epsilon). \tag{2.12}$$

Here the 4-momenta are all defined to flow into the vertex. We now discuss couplings of the $\mathbb{Z}_2$ odd Higgs bosons to fermions, which are relevant for the decay of the lightest $\mathbb{Z}_2$ odd Higgs boson. We define the fermions to be even under $\mathbb{Z}_2$, so in the $\mathbb{Z}_2$-symmetric limit, only Yukawa couplings involving H_1 are allowed. This is a "type I" 2-Higgs doublet model, which naturally avoids non-Standard Model flavor violation. When we include $\mathbb{Z}_2$ breaking, we must allow $O(\epsilon)$ Yukawa couplings to H_2, so this model is no longer type I for $\epsilon \neq 0$. We then have to worry about re-introducing unacceptably large flavor violation at $O(\epsilon)$. It may be interesting to consider the possibility that ϵ sufficiently suppresses non-Standard Model flavor violation. Our focus is on direct searches for new Higgs bosons, so we will avoid flavor problems by making the phenomenological assumption that all flavor breaking is contained in a single set of Yukawa coupling matrices y_u, y_d and y_e. This is "minimal flavor violation." Its validity depends on the UV completion of the theory having a single source of flavor breaking, at least to a very good approximation. With this assumption, the couplings of the Higgs fields to fermions is given by

$$\begin{aligned}\mathcal{L}_{\text{Yukawa}} = {} & (y_u)_{ij}\bar{Q}_{L_i}(H_1 + \epsilon_u H_2)u_{Rj} + (y_d)_{ij}\bar{Q}_{L_i}(H_1 + \epsilon_d H_2)d_{Rj} \\ & + (y_e)_{ij}\bar{L}_{L_i}(H_1 + \epsilon_e H_2)e_{Rj} + \text{h.c.}\end{aligned} \tag{2.13}$$

We will also make the phenomenological assumption that

$$\epsilon_u \simeq \epsilon_d \simeq \epsilon_e. \tag{2.14}$$

Then we have for any fermion f

$$g_{\phi^0 ff} = g_{hff}(\epsilon_{u,d,e} - \epsilon_h). \tag{2.15}$$

We see that the decays of ϕ^0, A and $H^\pm$ to fermions is controlled by the small parameter

$$\epsilon_f \equiv \epsilon_{u,d,e} - \epsilon_h. \tag{2.16}$$

JHEP09(2019)043

It is natural to assume that $\epsilon_f \sim \epsilon_V$. Note that both ϵ_V and ϵ_f involve ϵ_h, which depends on $\mathbb{Z}_2$ breaking in the Higgs potential. Therefore it is not natural to have $\epsilon_V \gg \epsilon_f$. If we have $\epsilon_f \gg \epsilon_V$, then fermion loops will induce $\mathbb{Z}_2$ breaking in the Higgs potential. For the top quark loop, we expect

$$\Delta m^2 \gtrsim \epsilon_t \frac{3y_t^2}{8\pi^2}\Lambda^2, \tag{2.17}$$

where Λ is a UV cutoff. Even for $\Lambda \sim$ TeV this is not suppressed.

Although we will assume $\epsilon_f \sim \epsilon_V$ in our study, the relative size of these suppressions is important for phenomenology because it determines the masses at which different decays become dominant. For example, if ϕ^0 is the lightest $\mathbb{Z}_2$ odd Higgs boson, it can decay either to WW or $b\bar{b}$. The decay to $b\bar{b}$ becomes dominant for $m_{\phi^0} \lesssim 2m_W$, but the precise mass for which this occurs is sensitive to the ratio

$$r = \frac{\epsilon_f}{\epsilon_V}. \tag{2.18}$$

Figure 4 shows branching ratios of the main decay modes of ϕ^0, A and $H^\pm$ to the SM particles for $r = 1/5$ and the dashed lines assume that $r = 5$. The phenomenology therefore depends on this parameter in addition to the spectrum of $\mathbb{Z}_2$ odd Higgs bosons. This parameter affects only the reach of a given search, so searches can be optimized only on the basis of the spectrum of masses of the exotic particles.

For all the benchmark models considered in our paper, we found parameters in the 2-Higgs doublet model parameter space that give an experimentally acceptable contribution to the S parameter. This is easily accomplished despite the fact that the additional Higgs bosons are light because they are approximately inert. In addition, these models easily satisfy all perturbativity constraints on the potential because the additional Higgs bosons are all light.[3]

3 Benchmark studies

In this section we study several benchmark models with multi-lepton signals. Simulated events for both signal and Standard Model backgrounds were generated by `MadGraph5` [32], with showering and hadronization simulated by `Pythia8` [33], and the detector response simulated by `Delphes3` [34]. The leading order cross-sections of the signal and Standard Model backgrounds for each channel are calculated by `MadGraph5`. Several of the Standard Model backgrounds, such as $t\bar{t}$ and W/Z+jets have large NLO contributions, therefore we scale the LO cross sections of these processes with their corresponding K-factors [35]. Since we focus on the final states that contain leptons and b jets, common selection requirements are applied to reconstructed jets, muons and electrons, before further selection requirements, optimized for each final state, are applied. Leptons are required to have a transverse momentum $p_T > 10$ GeV and pseudorapidity $|\eta| < 2.5$. We further require

[3] After fixing the values of ϵ and the masses of the additional scalars, we still have Δm^2 as a free parameter in the scalar potential, that can be adjusted in such a way that unitarity, perturbativity and stability of the potential is assured.

JHEP09(2019)043

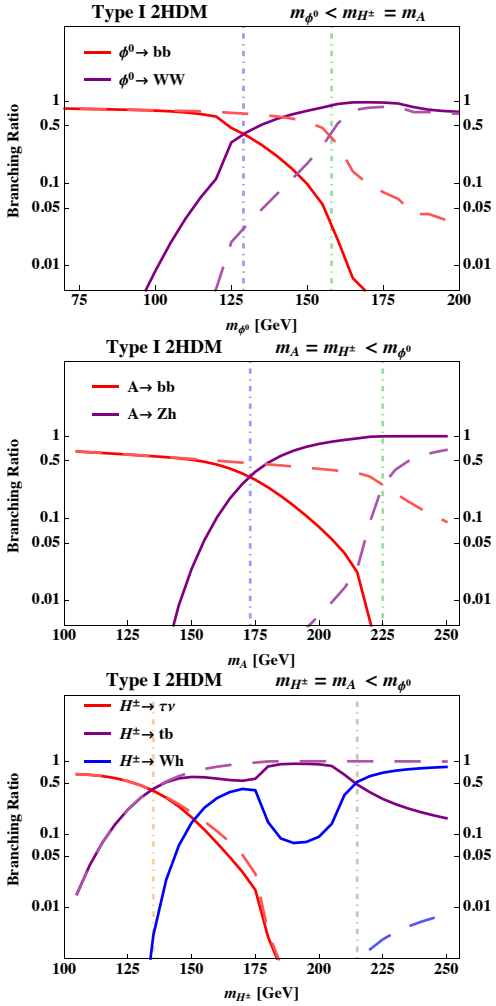

Figure 4. Branching Ratios of the main decay modes of ϕ^0, A and $H^\pm$ to the SM particles. The solid lines correspond to $r = 1/5$ and the dashed lines are for $r = 5$.

isolated leptons, as determined from the isolation ratio $R_{\rm iso} = p_{Tj}/p_{T\ell}$ where p_{Tj} is the clustered transverse energy, contained in a cone of radius ΔR around the lepton, and $p_{T\ell}$ is the lepton transverse energy. The lepton isolation requirement used in this analysis is $\Delta R < 0.2$ with $R_{\rm iso} < 0.09$. Similar isolation criteria have been used by ATLAS for their multilepton searches in LHC Run II [36].

Jets are required to satisfy $p_T > 20$ GeV and $|\eta| < 5$. The b-tagging efficiency is taken to be the same as the default setting in `Delphes3`. The remaining event selection is optimized for each individual channel, as described below.

3.1 3 leptons off Z peak

In the case when $\phi^0, H^\pm$ and A are all relatively heavy, they dominantly decay to final states that contain W or Z. In particular, $H^\pm(A)$ can decay to $W(Z)\phi^0$ or $W(Z)h$ depending on the mass splitting between ϕ^0 and $H^\pm(A)$. In this scenario, pair-produced non-Standard

JHEP09(2019)043

Benchmark 1	$(m_{\phi^0}, m_{A,H^\pm}) = (140, 170)$	$\epsilon_V = 5\epsilon_f = 0.1$	$\mathcal{BR}_{\phi^0 \to WW^*} \simeq 65\%$	$\mathcal{BR}_{H^\pm(A) \to W^*(Z^*)\phi^0} \simeq 100\%$
Benchmark 2	$(m_{\phi^0}, m_{A,H^\pm}) = (175, 175)$	$\epsilon_V = 5\epsilon_f = 0.1$	$\mathcal{BR}_{\phi^0 \to WW^*} \simeq 100\%$	$\mathcal{BR}_{H^\pm(A) \to W^*(Z^*)h} \simeq 40\%$
Benchmark 3	$(m_{\phi^0}, m_{A,H^\pm}) = (250, 210)$	$\epsilon_V = 5\epsilon_f = 0.001$	$\mathcal{BR}_{\phi^0 \to AZ^* \to (hZ)Z^*} \simeq 15\%$	$\mathcal{BR}_{\phi^0 \to H^\pm W^* \to (hW)W^*} \simeq 30\%$

Table 1. Details of the benchmarks for the 3 leptons off Z peak search.

Model H's can decay to five to six on- or off-shell vector bosons (figure 3a, 3b), therefore easily producing multiple leptons in the final state.

Asking for 3 light leptons has the advantage of a relatively low Standard Model background at LHC. Furthermore, given that pair produced $\phi^0 H^\pm$, $\phi^0 A$, $AH^\pm$ and H^+H^- may all contain 3 leptons in their final states, this channel also benefits from high signal multiplicities. Its drawback is that signal decays cannot be reconstructed, hence the signal kinematic features are not prominent enough to discriminate them against SM backgrounds. As a result, this channel basically becomes a lepton counting channel, which can be potentially covered by the 3- lepton bin of general multi-lepton searches from ATLAS and CMS.

Figure 5 shows the main result of this search, where we draw the 5σ contours reached at LHC run II and high-luminosity (HL) LHC. As we shall see, the overall 5σ reaches are not affected by varying ϵs as long as $\epsilon_f \ll \epsilon_V$. The reason is that for any values of the ϵs considered, the final states of the exotic H's decays always include combinations of the SM vector bosons and 125 GeV Higgs. In figure 2, we showed that the dominant decays for $A, \phi^0, H^\pm$ with smaller masses are to SM fermions, therefore they do not contribute to the multi-lepton signal.

Table 1 lists three benchmarks that are representative of each type of decay based on the assumptions on the mass hierarchy of ϕ^0, A and $H^\pm$. Benchmark 1 (B1) gives an example of the scenario in which $m_{\phi^0} < m_{H^\pm,A}$ and the mass splitting between ϕ^0 and $H^\pm(A)$ is sufficient to allow $H^\pm(A)$ to decay to $W^\pm(Z)\phi^0$. This corresponds to the region below the diagonal line in figure 5. Moving towards the diagonal, the mass splitting shrinks and the dominating decay modes of $H^\pm(A)$ are through $W^\pm(Z)h$, as long as $\epsilon_V > \epsilon_f$. Benchmark 2 (B2) corresponds to this region. Finally, as we cross the diagonal, where $m_{\phi^0} > m_{H^\pm,A}$, $\phi^0 \to H^\pm W^*$ or AZ^* can take over $\phi^0 \to VV$, provided ϵ_V is very small ($\lesssim 10^{-2}$). Even though ϕ^0's decay to $A(H^\pm)V^*$ is not kinematically favorable, it is not suppressed by ϵ_V. Benchmark 3 (B3) corresponds to this scenario.

The main Standard Model backgrounds include dibosons, $t\bar{t}V$, and $t\bar{t}$ or Z plus jets with one fake/non-prompt (FNP) lepton. To estimate the FNP leptons, we simulate Z plus jets and $t\bar{t}$, both of which are then decayed to include at least two leptons. Then, we select events that contain at least two reconstructed leptons and one jet, assuming a flat jet-faking-lepton rate. We match their contributions to the 3ℓ bin in figure 2(d) of the 36 fb^{-1} ATLAS multi-lepton search [36] and extract the jet-faking-lepton rate $\sim 8 \times 10^{-4}$.

For the preselections, we require a b-veto, at least 3 leptons with p_T of the leading (sub-leading) lepton $> 20\,(15)$ GeV. If a pair of OSSF leptons are found, we require that their invariant mass $\notin (m_Z - 15, m_Z + 15)$ GeV. Since the signals are relatively massive

JHEP09(2019)043

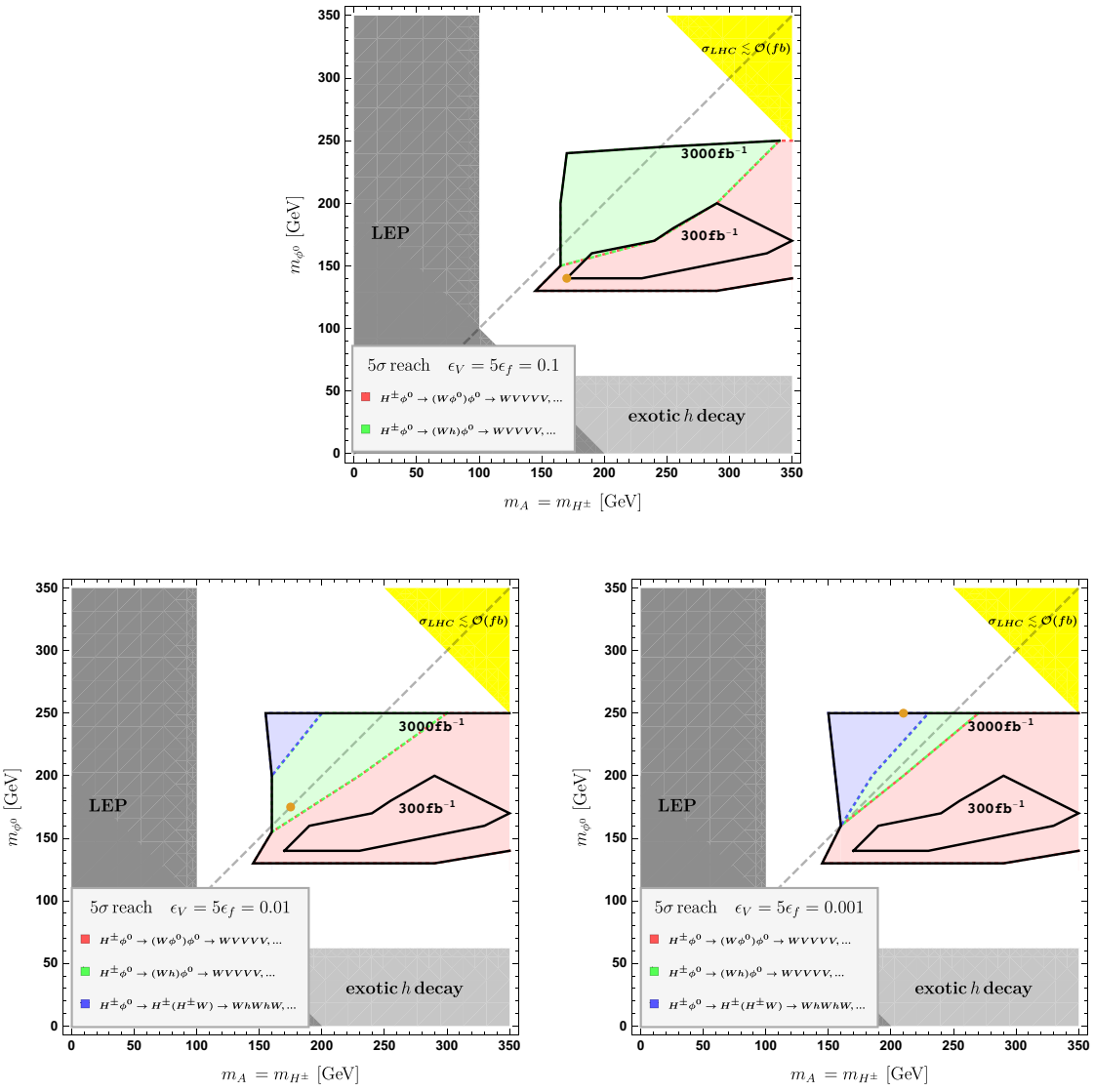

Figure 5. Five σ limits of the 3ℓ off Z channel for different values of ϵ_V at LHC 13 TeV. The signal region is defined by b-veto, $\not{E}_T > 40\,\text{GeV}$, $H_T > 300\,\text{GeV}$ and $N_j > 2$. The $3000\,\text{fb}^{-1}$ limit is further divided into three subregions where more than half of the signals come from each of the 'colored' decays. The three benchmaks described in the text are marked by orange dots.

and typically consist of five or six vector bosons, with more than half of them undergoing leptonic decays, we also require the missing energy $\not{E}_T > 40\,\text{GeV}$ and $H_T > 300\,\text{GeV}$, where H_T is the scalar sum of the lepton and jet p_T's.

Due to the limited number of signal events and their lack of prominent kinematic features, we are only able to place a final cut on the number of jets, N_j. Table 2 gives the signal yields for the three benchmarks and the SM backgrounds, assuming an integrated luminosity of $300\,\text{fb}^{-1}$. The signal corresponding to B1 is the only one that reach a 5σ

JHEP09(2019)043

significance for $300\,\text{fb}^{-1}$.[4] For B2 (B3), approximately $1700\,\text{fb}^{-1}$ ($3000\,\text{fb}^{-1}$) is required to achieve a 5σ significance. Compared to B1, B2 and B3 perform much worse, mainly because $h \to VV$ is not the dominant decay mode for a 125 GeV Higgs.

From the benchmark studies, it can be seen that in the case of a small $r(\equiv \epsilon_f/\epsilon_V)$ and large Higgs masses, ϕ^0, A and $H^\pm$ dominantly decay to $V + X$. Regardless of what assumptions are made about their mass hierarchy, the pair produced exotic Hs can always contribute to the signal 3ℓ off Z. We also investigate whether our results will be affected by varying the absolute values of ϵs. In figure 5, the 5σ contours are plotted for three different values of ϵ_V with r held fixed. As the ϵ's become smaller and smaller, the suppression due to ϵ^2 in the $\mathbb{Z}_2$-odd ϕ^0 decaying to SM fields becomes comparable to the phase space suppression of $\phi^0 \to H^\pm W^\mp$, and the latter starts to contribute to the signal region. Therefore, one sees a slight increase in the reach of the search as the ϵ's decrease. Despite that the dominant decays of ϕ^0, $H^\pm$ and A can be different under the variation of ϵ_V, they all end up contributing to the signals that we are looking for. As a result, the 5σ limit contour does not depend much on the absolute values of ϵ_V or ϵ_f. As long as ϵ_V is much larger than ϵ_f, the three types of decays compliment each other.

3.2 OSSF leptons with 3 b jets

The 3ℓ off Z search above targets the parameter space with relatively massive $\mathbb{Z}_2$ odd Higgs particles. In this section, we look at a relatively light ϕ^0 ($\lesssim 120\,\text{GeV}$), where $\phi^0 \to b\bar{b}$ becomes the dominant decay mode.

If $(m_{H^\pm} =) m_A > m_{\phi^0}$, A predominantly decays to $\phi^0 Z^{(*)}$. One interesting channel to consider is depicted in figure 3c, where $pp \to \phi^0 A \to \phi^0(\phi^0 Z^{(*)}) \to (b\bar{b})(b\bar{b}\ell^+\ell^-)$ gives a final state that consists of a pair of opposite-sign same-flavor (OSSF) leptons and four bs. Therefore, we ask for a pair of OSSF leptons with the leading (sub-leading) lepton $p_T > 20(15)\,\text{GeV}$, and at least 4 jets with 3 b-tagged jets. Since there is no invisible particles for the signal process, we also require $\not{E}_T < 50\,\text{GeV}$ as part of the preselections.

The dominating SM backgrounds are Z+jets, di-leptonic $t\bar{t}$ and single top production. Other SM backgrounds include di-bosons, Vh and fake/non-prompt leptons, but they are negligible compared to the first three SM processes [38].

Depending on whether the mass difference between A and ϕ^0 is greater than 91 GeV or not, this channel is further divided into the on- and off-shell Z signal regions. Below we give detailed benchmark studies focusing on each region. For both choice of benchmarks, we further assume that $r \equiv \epsilon_f/\epsilon_V = 5, \epsilon_f = 0.1$. Under these assumptions, $\mathcal{BR}_{\phi^0 \to b\bar{b}}$ is approximately 80% and $\mathcal{BR}_{A \to Z\phi^0}$ almost 100%.

3.2.1 Off Z : $(m_A, m_{\phi^0}) = (150, 70)\,\text{GeV}$

After applying the preselections discussed above, we try to reconstruct the entire decay chain for the signal. Since both ϕ^0s decay to $b\bar{b}$, we assume that the jet with the highest transverse momentum out of the non-b-tagged jets to be the fourth b. To reconstruct the ϕ^0s, we choose the combination of the jets that minimizes $(\Delta\phi_{j_1,j_2})^2 + (\Delta\phi_{j_3,j_4})^2$. Since A

[4] For the significance Z, we use the expression [37]: $Z = \sqrt{2\left[(S+B)\times\ln(1+S/B) - S\right]}$.

JHEP09(2019)043

	σ(fb)	initial@300fb^{-1}	pre-selection	final selection
$\mathbb{Z}_2$ odd Higgs $(m_{H^\pm,A}, m_{\phi^0})$				
Benchmark 1: $(170,140), \epsilon_V = 5\epsilon_f = 0.1$				
$\phi^0 H^\pm \to \phi^0(W^{\pm *}\phi^0), \phi^0 \to WW^*$	25	7478	41	23
$\phi^0 A \to \phi^0(Z^*\phi^0), \phi^0 \to WW^*$	14	4056	19	14
$H^\pm A \to (W^{\pm *}\phi^0)(Z^*\phi^0), \phi^0 \to WW^*$	15	4310	31	23
$H^+H^- \to (W^{+ *}\phi^0)(W^{- *}\phi^0), \phi^0 \to WW^*$	9	2535	24	18
B1 Total				78
Benchmark 2: $(175,175), \epsilon_V = 5\epsilon_f = 0.1$				
$\phi^0 H^\pm \to (W^+W^-)(W^{\pm *}h)$	18	5400	15	9
$\phi^0 A \to (W^+W^-)(Z^*h)$	10	3000	21	17
$H^\pm A \to (W^{\pm *}h)(Z^*h)$	7	2100	5	6
B2 Total				32
Benchmark 3: $(210,250), \epsilon_V = 5\epsilon_f = 0.001$				
$\phi^0 H^\pm \to (V^* H^\pm/A)(W^{\pm *}h)$	5	1500	7	6
$\phi^0 A \to (V^* H^\pm/A)(Z^*h)$	8	2400	7	7
$H^\pm A \to (W^{\pm *}h)(Z^*h)$	7	2100	12	11
B3 Total				24
Standard Model backgrounds:				
$W^\pm Z \to (\ell^\pm\nu)(\ell^+\ell^-)$	1300	3.9×10^5	190	44
ZZ, $Z\to\ell^+\ell^-$	124	3.7×10^4	24	9
$t\bar{t}V$	900	2.7×10^5	99	39
VVV	440	1.3×10^5	65	8
$hW, W\to\ell\nu$	6	1.8×10^3	13	3
di-leptonic $t\bar{t}$ (FNP)	7.8×10^4	2.3×10^7	196	95
di-leptonic tWj(FNP)	0.5×10^4	1.5×10^6	21	6
Z+jets, $Z\to\ell^+\ell^-$ (FNP)	2.3×10^6	6.9×10^8	85	13
di-leptonic WW (FNP)	1.0×10^4	2.9×10^6	22	3
SM Total				220

Table 2. Signal and the background yields for the channel 3ℓ off Z, assuming an integrated luminosity of 300 fb^{-1}. To estimate the number of events with FNP leptons, a flat jet-faking-lepton rate of 8×10^{-4} is used. The preselections are 3ℓ off Z, b-veto, $\not{E}_T > 40$ GeV, $H_T > 300$ GeV and the final selection is $N_j > 2$.

JHEP09(2019)043

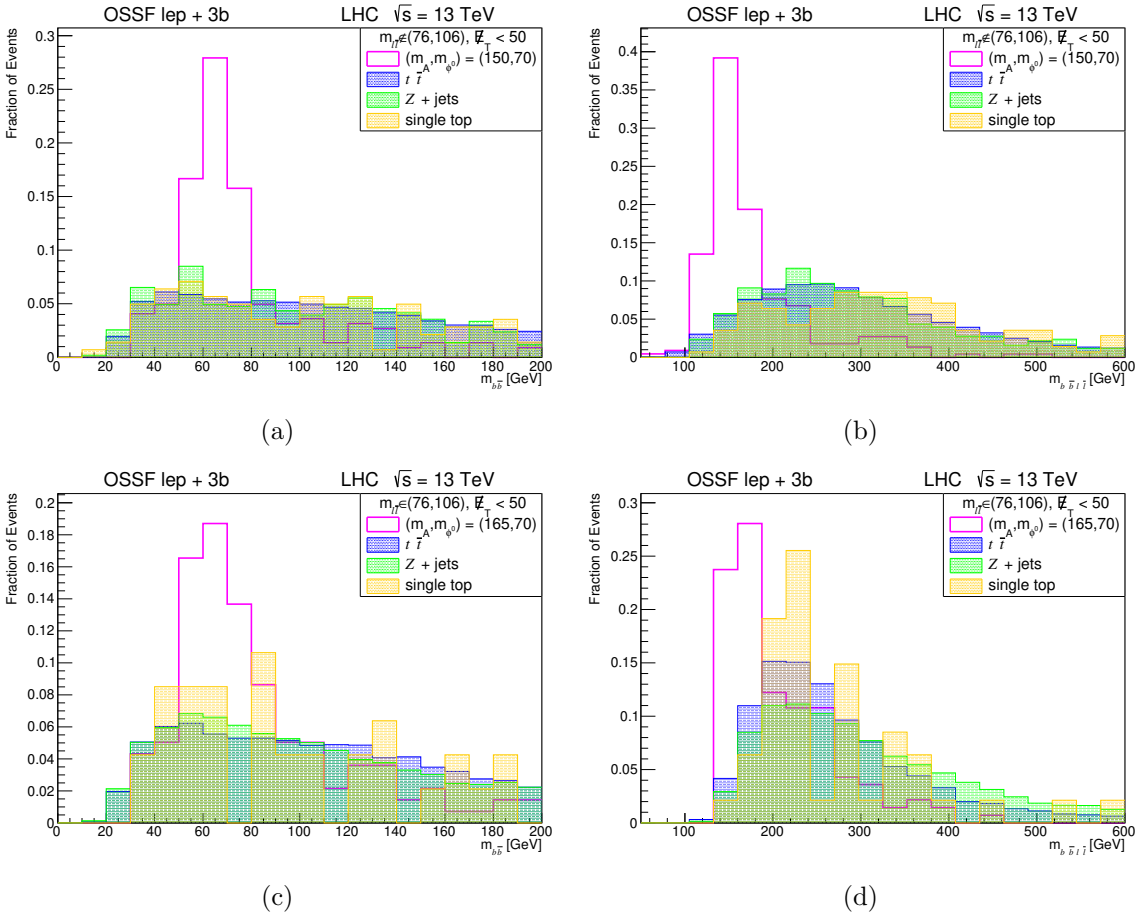

Figure 6. Distributions of $m_{b\bar{b}}$ and $m_{\ell^+\ell^- bb}$ for the OSSF leptons and $3b$ signal (section 3.2) and the main SM backgrounds after pre-selections. Both signal benchmarks have $r = 5, \epsilon_f = 0.1$. The preselections are OSSF ℓ pair off (on) Z, $N_j > 3$ with at least 3 b-tagged, $\not{E}_T < 50\,\text{GeV}$.

decays via ϕ^0 and $Z^{(*)}$, we then reconstruct A using the combination of the two leptons and the reconstructed ϕ^0 that has a smaller value in $|\Delta\phi|$. Figure 6 shows the reconstructed A and ϕ^0 mass distributions for signal and backgrounds after the preselections. As can be seen, both show prominent resonances for the signal, hence can be used to effectively suppress the backgrounds. The final selections are $\not{E}_T/\sqrt{H_T} < 2\,\text{GeV}^{1/2}$, $|m_{b\bar{b}} - m_{\phi^0}| < 15\,\text{GeV}$, $m_{b\bar{b}\ell\bar{\ell}} - m_A < 20\,\text{GeV}$. Table 3 gives the yields of the signal and the dominating backgrounds assuming an integrated luminosity of 300 fb^{-1}. To achieve a significance of 5σ, we need approximately $700\,\text{fb}^{-1}$.

3.2.2 On Z : $(m_A, m_{\phi^0}) = (165, 70)$ GeV

This benchmark produces an on-shell Z in its decay, therefore we apply the same pre-selections as before, except for requiring an on-shell Z instead of an off-shell Z. We repeat the analysis from section 3.2.1. The final selections are $\not{E}_T/\sqrt{H_T} < 2\,\text{GeV}^{1/2}$, $|m_{b\bar{b}} - m_{\phi^0}| < 20\,\text{GeV}$ and $|m_{b\bar{b}\ell\bar{\ell}} - m_A| < 10\,\text{GeV}$. Table 3 gives the signal and background yields assuming an integrated luminosity of 300 fb^{-1}. To achieve a significance of 5σ, we

JHEP09(2019)043

	σ(fb)	initial@300fb^{-1}	pre-selection		final selection	
$\mathbb{Z}_2$ odd Higgs (m_A, m_{ϕ^0}) $\phi^0 A \to \phi^0(\phi^0 Z) \to (b\bar{b})(b\bar{b}\ell^+\ell^-)$			B1	B2	B1	B2
Benchmark 1: (150,70)	10	3000	67	—	15	—
Benchmark 2: (165,70)	12	3600	—	50	—	12
SM Backgrounds						
di-leptonic $t\bar{t}$	78000	2.34×10^7	6554	1634	15	4
di-leptonic $tW+$ jets	4800	1.44×10^6	136	45	1	0
$Zb\bar{b}j, Z{\to}\ell^+\ell^-$	103500	3.11×10^7	185	3986	1	25
$Zbb\bar{b}\bar{b}, Z{\to}\ell^+\ell^-$	980	2.9×10^5	39	856	0	2
SM Total	—	—	—	—	17	31

Table 3. Signal and background yields for OSSF leptons plus 3 bs assuming an integrated luminosity of 300 fb^{-1}. The signal benchmarks both have $\epsilon_f = 5\epsilon_V = 0.1$. The preselections for Benchmark 1 (2) are OSSF ℓ pair off (on) Z, $N_j > 3$ with at least 3 b tagged and $\not{E}_T < 50$ GeV. The final selections for B1 and B2 are as described in the text above.

need roughly 1800 fb^{-1}. From the two benchmarks we studied, the on-shell Z case performs much worse compared to the off-shell Z case.

3.3 2 same-sign leptons

The search channel above targets a light ϕ^0. In this subsection, we consider a light $H^\pm(A)$. If $m_{\phi^0} > m_{H^\pm}(= m_A)$, $\phi^0 \to H^\pm W^{\mp(*)}$ or AZ^* become the dominant decay. If $H^\pm$ is lighter than 130 GeV, it decays to $\tau\nu$ predominantly. As depicted in figure 3d, where $pp \to \phi^0 H^\pm \to (H^\pm W^\mp) H^\pm$ with $H^\pm \to \tau\nu$, if W further decays leptonically, we can easily obtain a final state of $\ell^\pm\ell^\pm$ or $\tau_h^\pm\ell^\pm$, where ℓ represents e or μ and τ_h a τ-tagged jet.

For this search, we only consider the final states $\mu^\pm\mu^\pm$ or $\mu^\pm\tau_h^\pm$. $\tau_h^\pm\tau_h^\pm$ is not included because it suffers from a huge multi-jet background without light leptons. Electrons are not considered here because the charge misidentification is non-negligible for electrons. The benchmark we choose to work with is $(m_{\phi^0}, m_{H^\pm}) = (160, 110)$ GeV with $r = 1/5, \epsilon_V = 0.1$, where $\mathcal{BR}_{\phi^0 \to H^\pm W^\mp}$ is 80% approximately and $\mathcal{BR}_{H^\pm \to \tau\nu}$ 65% approximately.

The main irreducible backgrounds are dibosons, $t\bar{t}V$, VVV. The SM backgrounds with one fake/non-prompt (FNP) lepton or one fake τ_h come from W or Z plus jets and $t\bar{t}$. The fake rate is estimated to be approximately 10^{-4}.

For preselections, we ask for two same-sign muons or one muon plus one same-sign τ-tagged jet. Events that have any bs are vetoed. We further require that $\not{E}_T > 85$ GeV, because the signal has multiple invisible particles in its final state.

To combat the WZ and $W+$jets backgrounds, we look at the transverse mass of the W:

$$m_{\mathrm{T}}^W \equiv \sqrt{2p_T^\ell \not{p}_T (1 - \cos\Delta\phi_{\ell,\not{p}_T})}. \tag{3.1}$$

JHEP09(2019)043

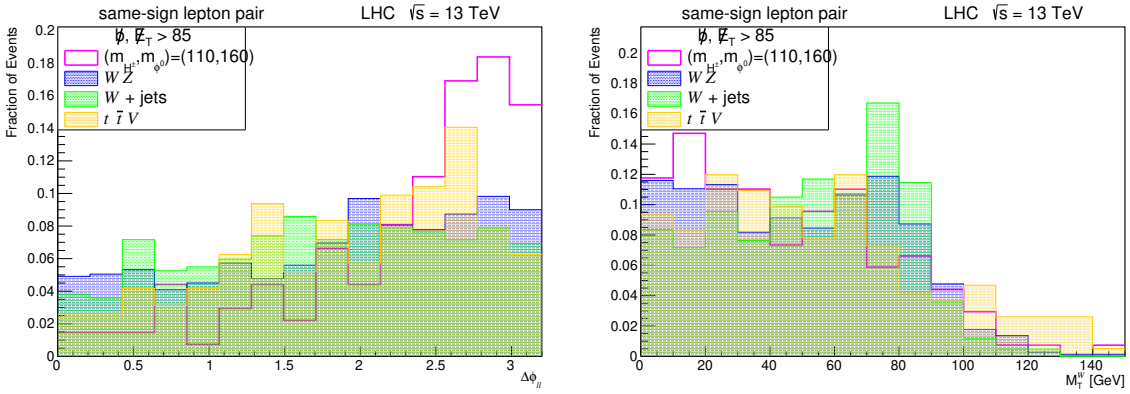

(a) (b)

Figure 7. Distributions of $\Delta\phi_{\ell\ell}$ and $m_{\rm T}^W$ for the SS lepton pair signal (section 3.3) and the main SM backgrounds after pre-selections. The signal benchmark is $(m_{H^\pm}, m_{\phi^0}) = (110, 160)\,\text{GeV}$ with $r = 1/5, \epsilon_V = 0.1$ The preselections are SS $\mu\mu$ or $\mu\tau_h$, b-veto and $\not{E}_T > 85\,\text{GeV}$.

Signal and SM processes	σ(fb)	initial@300fb^{-1}	pre-selection	final selection
$\phi^0 H^\pm \to (H^\pm W^\mp) H^\pm$, $H^\pm \to \tau\nu$	40	1.2×10^4	116	61
$W^\pm Z \to (\ell^\pm\nu)(\ell^+\ell^-)$	1300	3.9×10^5	599	116
ZZ, $Z \to \ell^+\ell^-$	124	3.7×10^4	35	14
$t\bar{t}V$	900	2.7×10^5	186	49
VVV	440	1.3×10^5	101	25
V+jets with V leptonically decay (FNP)	3.2×10^7	1.1×10^{10}	644	63
semi-/di-leptonic $t\bar{t}$ (FNP)	4.0×10^5	1.2×10^8	96	21
SM Total	—	—	—	288

Table 4. Signal and background yields for the same-sign leptons assuming an integrated luminosity $\mathcal{L} = 300\,\text{fb}^{-1}$. To estimate the FNP leptons, we use a flat fake rate to be $\sim 10^{-4}$. The signal benchmark is that $m_{H^\pm} = 110\,\text{GeV}$, $m_{\phi^0} = 160\,\text{GeV}$ and $r = 1/5, \epsilon_V = 0.1$. The preselections are SS $\mu\mu$ or $\mu\tau_h$, b-veto and $\not{E}_T > 85\,\text{GeV}$. The final selections are $7 > N_j > 2$, $\Delta\phi_{\ell\ell} > 2.1$ and $|m_{\rm T}^W - m_W| > 5\,\text{GeV}$.

Since there are two leptons, we reconstruct $m_{\rm T}^W$ for both of them and take the smaller one to be $m_{\rm T}^W$. Based on the kinematic distributions plotted in figure 7, the final selections comprise $7 > N_j > 2$, $\Delta\phi_{\ell\ell} > 2.1$ and $|m_{\rm T}^W - m_W| > 5\,\text{GeV}$. Table 4 gives the yields of the signal and background processes assuming an integrated luminosity of $300\,\text{fb}^{-1}$. To get 5σ, an integrated luminosity of 600fb^{-1} is required.

4 Conclusions

In this paper we considered the phenomenology of a 2-Higgs doublet model where the additional Higgs bosons are almost inert. This means that there is an approximate $\mathbb{Z}_2$ symmetry that ensures that there is a Standard Model-like Higgs boson mass eigenstate

JHEP09(2019)043

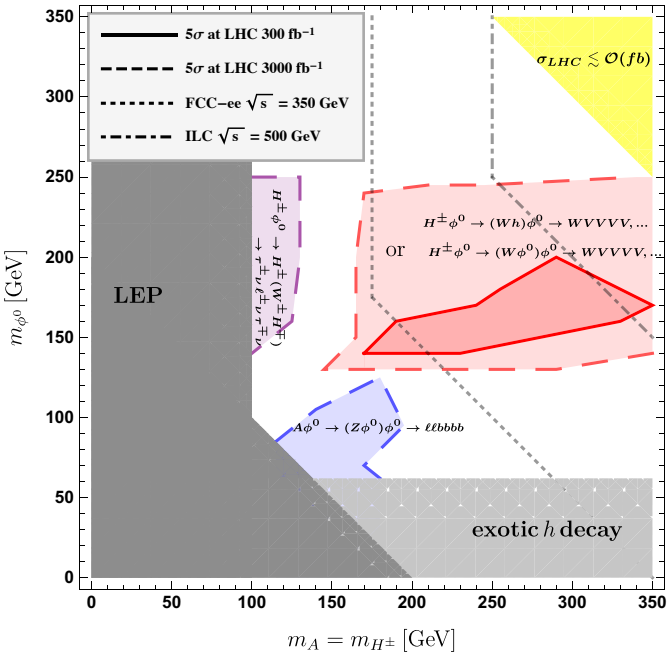

Figure 8. The dashed (solid) lines are the 5σ reach for an integrated luminosity of 3000fb^{-1} (300fb^{-1}) at LHC Run II. For the OSSFℓ-plus-$3b$ (blue) search, $r \equiv \epsilon_f/\epsilon_V = 5$ is chosen. For the 2 SSℓ (purple) and the 3ℓ off Z (red) searches, $r = 1/5$ is chosen. The regions for LEP, FCC-ee, and ILC are the kinematically available regions, so they correspond to the maximal possible reach.

Signal	Main Decay Modes	Final States	$\mathcal{L}_{5\sigma}(\text{fb}^{-1})$
$\phi^0 A$	$(b\bar{b})(\phi^0 Z^*) \to (b\bar{b})(b\bar{b}\ell^+\ell^-)$	OSSF+$3b$	300 (section 3.2)
	$(WW^*)(\phi^0 Z^*) \to (WW^*)(WW^*Z^*)$	3 leptons	300 (section 3.1)
$\phi^0 H^\pm$	$(b\bar{b})(\phi^0 W^*) \to (b\bar{b})(b\bar{b}\ell^+\nu)$	$1\ell + 3b$	killed by W+jets
	$(WW^*)(\phi^0 W^*) \to (WW^*)(WW^*W^*)$	3 leptons	300 (section 3.1)
$AH^\pm$	$(\phi^0 Z^*)(\phi^0 W^*) \to (b\bar{b}Z^*)(b\bar{b}W^*)$	2 SSL+$3b$	killed by $t\bar{t}$
	$(\phi^0 Z^*)(\phi^0 W^*) \to (WW^*Z^*)(WW^*W^*)$	3 leptons	300 (section 3.1)
H^+H^-	$(\phi^0 W^*)(\phi^0 W^*) \to (b\bar{b}W^*)(b\bar{b}W^*)$	$2\ell + 3b$	killed by $t\bar{t}$, Z+jets
	$(\phi^0 W^*)(\phi^0 W^*) \to (WW^*W^*)(WW^*W^*)$	3 leptons	300 (section 3.1)

Table 5. Plausible channels assuming that $m_A = m_{H^\pm} > m_\phi$ and that $A, H^\pm$ undergo electroweak cascade decays. SSL means same-sign leptons. OSSF means opposite-sign same-flavor lepton pair.

whose VEV is dominantly responsible for the masses of Standard Model vector bosons and fermions. This fully explains the agreement of the couplings of the observed 125 GeV Higgs boson, while allowing the additional Higgs bosons to be light and therefore kinematically accessible at the LHC. The phenomenology of this kind of model is very distinctive. The $\mathbb{Z}_2$ odd Higgs bosons are pair produced by electroweak interactions, and undergo cascade decays with the heaviest Standard Model states at the end of the decay chain.

JHEP09(2019)043

Signal	Main Decay Modes	Final States	$\mathcal{L}_{5\sigma}(\text{fb}^{-1})$
$\phi^0 A$	$(AZ^*)A \to (b\bar{b}\ell^+\ell^-)(b\bar{b})$	OSSF+3b	signal σ too small
	$(H^\pm W^*)A \to (\tau\nu W^*)(b\bar{b})$	$2\ell + 2b$	killed by $t\bar{t}$
	$(H^\pm W^*)A \to (tbW^*)(b\bar{b})$	$2\ell + 3b$	killed by $t\bar{t}$
$\phi^0 H^\pm$	$(H^\pm W^*)H^\pm$, $H^\pm \to \tau^\pm\nu$	2SSL	2250 (section 3.3)
	$(H^\pm W^*)H^\pm \to (tbW^*)(t\bar{b})$	2SSL+2b	signal σ too small
	$(AZ^*)H^\pm \to (b\bar{b}Z^*)(\tau^\pm\nu)$	2SSL+2b	signal σ too small

Table 6. Plausible channels assuming that $m_A = m_{H^\pm} < m_{\phi^0}$ and that ϕ^0 undergoes electroweak cascade decays. SSL means same-sign lepton pairs. OSSF means opposite-sign same-flavor lepton pair.

Signal	Main Decay Modes	Final States	$\mathcal{L}_{5\sigma}(\text{fb}^{-1})$
$A\phi^0$	$(b\bar{b})(b\bar{b})$	4b	killed by QCD
	$(Z^*h)(WW^*)\to(Z^*b\bar{b})(WW^*)$	2SSL+2b	killed by $t\bar{t}$, σ too small
	$(Z^*h)(WW^*)\to(Z^*VV^*)(WW^*)$	3 leptons	2000 (section 3.1)
$AH^\pm$	$(b\bar{b})(\tau\nu)$	$1\ell+2b$	killed by W+jets
	$(Z^*h)(W^*h)\to(Z^*b\bar{b})(W^*b\bar{b})$	2SSL+2-3b	signal σ too small
	$(Z^*h)(W^*h)\to(Z^*VV^*)(W^*VV^*)$	3 leptons	2000 (section 3.1)
$\phi^0 H^\pm$	$(b\bar{b})(\tau\nu)$	$1\ell+2b$	killed by $t\bar{t}$, W+jets
	$(W^*W)(t^*\bar{b})$	2SSL+2b	killed by $t\bar{t}$
	$(W^*W)(W^*h)\to(W^*W)(W^*b\bar{b})$	2SSL+2b	killed by $t\bar{t}$, σ too small
	$(W^*W)(W^*h)\to(W^*W)(W^*VV^*)$	3 leptons	2000 (section 3.1)
H^+H^-	$(cs)(\tau\nu)$	$1\ell+2j$	killed by W+jets
	$(\bar{t}^*b)(t^*\bar{b})$	$2\ell+2b$	killed by $t\bar{t}$, Z+jets
	$(W^{+*}h)(W^{-*}h)\to(W^{+*}b\bar{b})(W^{-*}b\bar{b})$	2SSL+2-3b	signal σ too small
	$(W^{+*}h)(W^{-*}h)\to(W^{+*}VV^*)(W^{-*}VV^*)$	3 leptons	signal σ too small

Table 7. Plausible channels assuming that $A, H^\pm, \phi^0$ undergo non-cascade decays. SSL means same-sign leptons.

In this paper we initiated the exploration of the phenomenology of this class of models. We focused on LHC searches, and showed that these are sensitive despite the low production cross sections. The results of the investigation are summarized in tables 5, 6, and 7. The most effective searches are multi-lepton searches, but custom searches involving leptons and b jets are also effective. Figure 8 summarizes our results. We show the 5σ reach for each search for an LHC integrated luminosity of $3000\,\text{fb}^{-1}$ (dashed) and $300\,\text{fb}^{-1}$ (solid). We also compare the bounds with those from future e^+e^- colliders, which will be both clean in the background and efficient in producing the types of signals we study here. We conclude that the high luminosity LHC can explore a significant region of the parameter space of these well-motivated models.

JHEP09(2019)043

Acknowledgments

This work was supported in part by the DOE under grant DE-SC-000999. N.N. was supported by FONDECYT (Chile) grant 3170906 and in part by Conicyt PIA/Basal FB0821.

A Almost inert Higgs in 2HDM

The purpose of this note is to make contact with the conventions adopted in 2HDM literature. Here we are going to use the mixing angles ϵ_V and ϵ_f, where the notation is just a reminder that these angles are small.

The two Higgs doublet model (2HDM) extends the Standard Model (SM) Higgs sector by allowing two complex doublets. Without loss of generality, we choose to work with the Higgs basis, where only one of the doublets get a non-zero vacuum expectation value (VEV) after the electroweak symmetry breaking (EWSB). The fields can be parametrized around their VEVs as

$$\begin{aligned} \mathcal{H}_1 &= \begin{pmatrix} G^+ \\ \frac{1}{\sqrt{2}}(v + h_1^0 + iG^0) \end{pmatrix}, \\ \mathcal{H}_2 &= \begin{pmatrix} H^+ \\ \frac{1}{\sqrt{2}}(h_2^0 + iA) \end{pmatrix}. \end{aligned} \tag{A.1}$$

The CP-even mass eigenstates are formed by linear combinations of h_1^0, h_2^0. Defining the mixing angle to be ϵ_V,

$$\begin{pmatrix} h \\ \phi^0 \end{pmatrix} = \begin{pmatrix} \cos\epsilon_V & \sin\epsilon_V \\ -\sin\epsilon_V & \cos\epsilon_V \end{pmatrix} \begin{pmatrix} h_1^0 \\ h_2^0 \end{pmatrix}, \tag{A.2}$$

where h is the observed 125 GeV Higgs boson and ϕ^0 the additional neutral scalar. The couplings of the neutral Higgs bosons to vector bosons are all related to ϵ_V. For example:

$$\begin{aligned} hAZ &\propto \sin\epsilon_V, & \phi^0 AZ &\propto \cos\epsilon_V, \\ hH^\mp W^\pm &\propto \sin\epsilon_V, & \phi^0 H^\mp W^\pm &\propto \cos\epsilon_V, \\ hZZ &\propto \cos\epsilon_V, & \phi^0 ZZ &\propto \sin\epsilon_V. \end{aligned} \tag{A.3}$$

In the limit that $\epsilon_V \to 0$, the hZZ coupling becomes SM-like, and $\mathcal{H}_1$ behaves just as the SM doublet in terms of its gauge couplings.

The Yukawa sector of 2HDM can be written as

$$-\mathcal{L}_{yuk} = \overline{Q}_{L_i} y_u^{ij} u_{R_j} \tilde{H}_u + \overline{Q}_{L_i} y_d^{ij} d_{R_j} H_d + \overline{L}_{L_i} y_e^{ij} e_{R_j} H_l + h.c., \tag{A.4}$$

where i, j are quark flavor indices and H_u, H_d, H_l are linear combinations of $\mathcal{H}_1$ and $\mathcal{H}_2$. The mixing of $\mathcal{H}_1$ and $\mathcal{H}_2$ in H_u, H_d, H_l can not be arbitrary, due to the fact that tree-level flavor changing neutral currents (FCNC) are observed to be very rare. To suppress FCNCs,

JHEP09(2019)043

what is conventionally done is to impose a $\mathbb{Z}_2$ symmetry to all the SM fermions and H_u, H_d, H_l. The $\mathbb{Z}_2$ basis is related to the Higgs basis in the following way:

$$\begin{pmatrix} \mathcal{H}_1 \\ \mathcal{H}_2 \end{pmatrix} = \begin{pmatrix} \cos\beta & \sin\beta \\ -\sin\beta & \cos\beta \end{pmatrix} \begin{pmatrix} \Phi_1 \\ \Phi_2 \end{pmatrix}, \tag{A.5}$$

where $\Phi_1 \to -\Phi_1$, $\Phi_2 \to +\Phi_2$ under a $\mathbb{Z}_2$ transformation, and $\tan\beta = \langle\Phi_2\rangle_0 / \langle\Phi_1\rangle_0$. Depending on how the fermions transform under $\mathbb{Z}_2$, there arise several 'types' of 2HDM.

The simplest version (type I) is to let all the SM fields even under $\mathbb{Z}_2$. Therefore, in type I, only $\Phi_2 (= H_u = H_d = H_l)$ can participate in the Yukawa interactions. Suppose the mixing angle between $\mathcal{H}_1$ and $\mathcal{H}_2$ that makes up Φ_2 is

$$\epsilon_f \equiv \pi/2 - \beta. \tag{A.6}$$

Together with ϵ_V, the couplings of the neutral Higgs bosons to the SM fermions can all be determined:

$$hf\bar{f} \propto \cos(\epsilon_f - \epsilon_V)/\cos\epsilon_f, \qquad \phi^0 f\bar{f} \propto \sin(\epsilon_f - \epsilon_V)/\cos\epsilon_f, \qquad Af\bar{f} \propto \tan\epsilon_f. \tag{A.7}$$

In the small ϵ_f limit (that corresponds to large $\tan\beta$) $\mathcal{H}_2$'s interactions with the SM fermions are suppressed, and $\mathcal{H}_1$ acts as the SM Higgs doublet in the Yukawa sector. From eq. (A.5) we can see that $\mathcal{H}_{1,2} = \Phi_{2,1}$ for $\epsilon_f \to 0$. In this limit, and only when all sources of $\mathbb{Z}_2$ breaking are zero (all $\epsilon s \to 0$) the approximate $\mathbb{Z}_2$-basis from eq. (2.6) corresponds to the Higgs basis.

Following the conventions in [7, 39–41], the mixing angle of the CP even states in the $\mathbb{Z}_2$ basis (Φ_1,Φ_2) is defined to be α, where

$$\begin{pmatrix} \phi^0_{\text{heavy}} \\ \phi^0_{\text{light}} \end{pmatrix} = \begin{pmatrix} \cos\alpha & \sin\alpha \\ -\sin\alpha & \cos\alpha \end{pmatrix} \begin{pmatrix} \sqrt{2}\text{Re}\Phi^0_1 - v_1 \\ \sqrt{2}\text{Re}\Phi^0_2 - v_2 \end{pmatrix}. \tag{A.8}$$

Eq. (A.8) together with eqs. (A.1) and (A.5) yield:

$$\begin{pmatrix} \phi^0_{\text{heavy}} \\ \phi^0_{\text{light}} \end{pmatrix} = \begin{pmatrix} \cos(\alpha-\beta) & \sin(\alpha-\beta) \\ -\sin(\alpha-\beta) & \cos(\alpha-\beta) \end{pmatrix} \begin{pmatrix} h^0_1 \\ h^0_2 \end{pmatrix}. \tag{A.9}$$

Comparing eq. (A.9) with (A.2), we see that if ϕ^0_{light} is identified with the 125 GeV Higgs h, then $\epsilon_V \equiv \pi/2 - (\beta - \alpha)$; if ϕ^0_{heavy} is identified with h, then $\epsilon_V \equiv -(\beta - \alpha)$.

To get an almost inert Higgs sector, both the gauge couplings and Yukawa couplings of the field are set to be SM-like, i.e.

$$\epsilon_V \equiv \pi/2 - (\beta - \alpha) \ \ [\text{or} - (\beta - \alpha)] \to 0, \quad \epsilon_f \equiv \pi/2 - \beta \to 0. \tag{A.10}$$

Therefore, we are interested in the large $\tan\beta$ limit of the type I 2HDM. There are very few experimental constraints in this limit.

JHEP09(2019)043

$c\tau$(mm)		$m_{H^\pm}$(GeV)					
		150	170	190	210	230	250
ϵ_V	10^{-1}	2.7×10^{-4}	4.2×10^{-5}	1.0×10^{-6}	2.0×10^{-7}	4.2×10^{-8}	1.8×10^{-8}
	10^{-2}	2.7×10^{-2}	4.2×10^{-3}	1.0×10^{-4}	2.0×10^{-5}	4.2×10^{-6}	1.8×10^{-6}
	10^{-3}	2.7	4.2×10^{-1}	1.0×10^{-2}	2.0×10^{-3}	4.2×10^{-4}	1.8×10^{-4}
	10^{-4}	2.7×10^{2}	4.2×10^{1}	1.0	2.0×10^{-1}	4.2×10^{-2}	1.8×10^{-2}
	10^{-5}	2.7×10^{4}	4.2×10^{3}	1.0×10^{2}	2.0×10^{1}	4.2	1.8
	10^{-6}	2.7×10^{6}	4.2×10^{5}	1.0×10^{4}	2.0×10^{3}	4.2×10^{2}	1.8×10^{2}

Table 8. $c\tau$ in millimeters for different values of $\epsilon_V (= 5\epsilon_f)$ and the charged Higgs mass ($m_{H^\pm}$).

Expanding the kinetic terms for $\mathcal{H}_2$, we obtain terms like

$$\frac{1}{2}\sqrt{g^2+g'^2}Z_\mu(-\partial^\mu\phi^0 A + \partial^\mu A\phi^0), \tag{A.11}$$

$$\frac{i}{2}\sqrt{g^2+g'^2}(c_W^2 - s_W^2)Z_\mu(\partial^\mu H^- H^+ - H^-\partial^\mu H^+), \tag{A.12}$$

$$-\frac{ig}{2}W_\mu^+(\partial^\mu H^-\phi^0 - H^-\partial^\mu\phi^0) + h.c., \tag{A.13}$$

$$\frac{g}{2}W_\mu^+(-\partial^\mu H^- A + H^-\partial^\mu A) + h.c. \tag{A.14}$$

Therefore, the electroweak pair production of non-SM Higgs fields is not suppressed in this limit, which we will exploit in our search.

Finally, in table 8, we show the value of $c\tau$ for different values of $\epsilon_V (= 5\epsilon_f)$ and the charged Higgs mass ($m_{H^\pm}$).

References

[1] ATLAS collaboration, *Observation of a new particle in the search for the Standard Model Higgs boson with the ATLAS detector at the LHC*, *Phys. Lett.* **B 716** (2012) 1 [arXiv:1207.7214] [INSPIRE].

[2] CMS collaboration, *Observation of a new boson at a mass of 125 GeV with the CMS experiment at the LHC*, *Phys. Lett.* **B 716** (2012) 30 [arXiv:1207.7235] [INSPIRE].

[3] ATLAS and CMS collaborations, *Measurements of the Higgs boson production and decay rates and constraints on its couplings from a combined ATLAS and CMS analysis of the LHC pp collision data at $\sqrt{s} = 7$ and 8 TeV*, *JHEP* **08** (2016) 045 [arXiv:1606.02266] [INSPIRE].

[4] ATLAS collaboration, *Combined measurements of Higgs boson production and decay using up to 80 fb^{-1} of proton-proton collision data at $\sqrt{s} = 13$ TeV collected with the ATLAS experiment*, ATLAS-CONF-2018-031, CERN, Geneva, Switzerland (2018).

JHEP09(2019)043

[5] CMS collaboration, *Combined measurements of Higgs boson couplings in proton-proton collisions at* $\sqrt{s} = 13$ *TeV*, *Eur. Phys. J.* **C 79** (2019) 421 [arXiv:1809.10733] [INSPIRE].

[6] H.E. Haber and Y. Nir, *Multiscalar models with a high-energy scale*, *Nucl. Phys.* **B 335** (1990) 363 [INSPIRE].

[7] J.F. Gunion and H.E. Haber, *The CP conserving two Higgs doublet model: the approach to the decoupling limit*, *Phys. Rev.* **D 67** (2003) 075019 [hep-ph/0207010] [INSPIRE].

[8] CMS collaboration, *Search for an exotic decay of the Higgs boson to a pair of light pseudoscalars in the final state with two muons and two b quarks in pp collisions at* 13 *TeV*, *Phys. Lett.* **B 795** (2019) 398 [arXiv:1812.06359] [INSPIRE].

[9] ATLAS collaboration, *Search for Higgs boson decays into a pair of light bosons in the* $bb\mu\mu$ *final state in pp collision at* $\sqrt{s} = 13$ *TeV with the ATLAS detector*, *Phys. Lett.* **B 790** (2019) 1 [arXiv:1807.00539] [INSPIRE].

[10] CMS collaboration, *Search for invisible decays of a Higgs boson produced through vector boson fusion in proton-proton collisions at* $\sqrt{s} = 13$ *TeV*, *Phys. Lett.* **B 793** (2019) 520 [arXiv:1809.05937] [INSPIRE].

[11] ATLAS collaboration, *Combination of searches for invisible Higgs boson decays with the ATLAS experiment*, *Phys. Rev. Lett.* **122** (2019) 231801 [arXiv:1904.05105] [INSPIRE].

[12] N. Craig, J. Galloway and S. Thomas, *Searching for signs of the second Higgs doublet*, arXiv:1305.2424 [INSPIRE].

[13] A. Delgado, G. Nardini and M. Quirós, *A light supersymmetric Higgs sector hidden by a Standard Model-like Higgs*, *JHEP* **07** (2013) 054 [arXiv:1303.0800] [INSPIRE].

[14] M. Carena, I. Low, N.R. Shah and C.E.M. Wagner, *Impersonating the Standard Model Higgs boson: alignment without decoupling*, *JHEP* **04** (2014) 015 [arXiv:1310.2248] [INSPIRE].

[15] N.G. Deshpande and E. Ma, *Pattern of symmetry breaking with two Higgs doublets*, *Phys. Rev.* **D 18** (1978) 2574 [INSPIRE].

[16] I.F. Ginzburg, K.A. Kanishev, M. Krawczyk and D. Sokolowska, *Evolution of universe to the present inert phase*, *Phys. Rev.* **D 82** (2010) 123533 [arXiv:1009.4593] [INSPIRE].

[17] E. Ma, *Verifiable radiative seesaw mechanism of neutrino mass and dark matter*, *Phys. Rev.* **D 73** (2006) 077301 [hep-ph/0601225] [INSPIRE].

[18] R. Barbieri, L.J. Hall and V.S. Rychkov, *Improved naturalness with a heavy Higgs: an alternative road to LHC physics*, *Phys. Rev.* **D 74** (2006) 015007 [hep-ph/0603188] [INSPIRE].

[19] L. Lopez Honorez, E. Nezri, J.F. Oliver and M.H.G. Tytgat, *The inert doublet model: an archetype for dark matter*, *JCAP* **02** (2007) 028 [hep-ph/0612275] [INSPIRE].

[20] A. Goudelis, B. Herrmann and O. Stål, *Dark matter in the inert doublet model after the discovery of a Higgs-like boson at the LHC*, *JHEP* **09** (2013) 106 [arXiv:1303.3010] [INSPIRE].

[21] A. Arhrib, Y.-L.S. Tsai, Q. Yuan and T.-C. Yuan, *An updated analysis of inert Higgs doublet model in light of the recent results from LUX, PLANCK, AMS-02 and LHC*, *JCAP* **06** (2014) 030 [arXiv:1310.0358] [INSPIRE].

[22] A. Ilnicka, M. Krawczyk and T. Robens, *Inert doublet model in light of LHC run I and astrophysical data*, *Phys. Rev.* **D 93** (2016) 055026 [arXiv:1508.01671] [INSPIRE].

[23] A. Ilnicka, T. Robens and T. Stefaniak, *Constraining extended scalar sectors at the LHC and beyond*, *Mod. Phys. Lett.* **A 33** (2018) 1830007 [arXiv:1803.03594] [INSPIRE].

JHEP09(2019)043

[24] A. Belyaev, G. Cacciapaglia, I.P. Ivanov, F. Rojas-Abatte and M. Thomas, *Anatomy of the inert two Higgs doublet model in the light of the LHC and non-LHC dark matter searches*, *Phys. Rev.* **D 97** (2018) 035011 [arXiv:1612.00511] [INSPIRE].

[25] J. Kalinowski, W. Kotlarski, T. Robens, D. Sokolowska and A.F. Zarnecki, *Benchmarking the inert doublet model for e^+e^- colliders*, *JHEP* **12** (2018) 081 [arXiv:1809.07712] [INSPIRE].

[26] ATLAS collaboration, *Search for long-lived particles in final states with displaced dimuon vertices in pp collisions at $\sqrt{s} = 13$ TeV with the ATLAS detector*, *Phys. Rev.* **D 99** (2019) 012001 [arXiv:1808.03057] [INSPIRE].

[27] CMS collaboration, *Search for long-lived charged particles in proton-proton collisions at $\sqrt{s} = 13$ TeV*, *Phys. Rev.* **D 94** (2016) 112004 [arXiv:1609.08382] [INSPIRE].

[28] CMS collaboration, *Search for heavy stable charged particles with 12.9 fb^{-1} of 2016 data*, CMS-PAS-EXO-16-036, CERN, Geneva, Switzerland (2016).

[29] ALEPH, DELPHI, L3, OPAL and LEP Working Group for Higgs Boson Searches collaborations, *Search for neutral MSSM Higgs bosons at LEP*, *Eur. Phys. J.* **C 47** (2006) 547 [hep-ex/0602042] [INSPIRE].

[30] ALEPH, DELPHI, L3, OPAL and LEP collaborations, *Search for charged Higgs bosons: combined results using LEP data*, *Eur. Phys. J.* **C 73** (2013) 2463 [arXiv:1301.6065] [INSPIRE].

[31] A. Arbey, F. Mahmoudi, O. Stal and T. Stefaniak, *Status of the charged Higgs boson in two Higgs doublet models*, *Eur. Phys. J.* **C 78** (2018) 182 [arXiv:1706.07414] [INSPIRE].

[32] J. Alwall et al., *The automated computation of tree-level and next-to-leading order differential cross sections and their matching to parton shower simulations*, *JHEP* **07** (2014) 079 [arXiv:1405.0301] [INSPIRE].

[33] T. Sjöstrand et al., *An introduction to PYTHIA* 8.2, *Comput. Phys. Commun.* **191** (2015) 159 [arXiv:1410.3012] [INSPIRE].

[34] DELPHES 3 collaboration, *DELPHES* 3*, a modular framework for fast simulation of a generic collider experiment*, *JHEP* **02** (2014) 057 [arXiv:1307.6346] [INSPIRE].

[35] J.M. Campbell, R.K. Ellis and C. Williams, *Vector boson pair production at the LHC*, *JHEP* **07** (2011) 018 [arXiv:1105.0020] [INSPIRE].

[36] ATLAS collaboration, *Search for supersymmetry in final states with two same-sign or three leptons and jets using 36 fb^{-1} of $\sqrt{s} = 13$ TeV pp collision data with the ATLAS detector*, *JHEP* **09** (2017) 084 [arXiv:1706.03731] [INSPIRE].

[37] G. Cowan, K. Cranmer, E. Gross and O. Vitells, *Asymptotic formulae for likelihood-based tests of new physics*, *Eur. Phys. J.* **C 71** (2011) 1554 [*Erratum ibid.* **C 73** (2013) 2501] [arXiv:1007.1727] [INSPIRE].

[38] ATLAS collaboration, *Measurement of VH, $H \to b\bar{b}$ production as a function of the vector-boson transverse momentum in* 13 TeV *pp collisions with the ATLAS detector*, *JHEP* **05** (2019) 141 [arXiv:1903.04618] [INSPIRE].

[39] J. Bernon, J.F. Gunion, H.E. Haber, Y. Jiang and S. Kraml, *Scrutinizing the alignment limit in two-Higgs-doublet models: $m_h = 125$ GeV*, *Phys. Rev.* **D 92** (2015) 075004 [arXiv:1507.00933] [INSPIRE].

[40] G.C. Branco, P.M. Ferreira, L. Lavoura, M.N. Rebelo, M. Sher and J.P. Silva, *Theory and phenomenology of two-Higgs-doublet models*, *Phys. Rept.* **516** (2012) 1 [arXiv:1106.0034] [INSPIRE].

[41] J.F. Gunion, H.E. Haber, G.L. Kane and S. Dawson, *The Higgs hunter's guide*, *Front. Phys.* **80** (2000) 1 [INSPIRE].

JHEP09(2019)043